Chapter 2

Erbium-Doped Fiber Amplifiers - Basics

2.1 Fundamental properties of EDFA [2.1],[2.2]

2.1.1 Emission and absorption cross sections

Rare-earth-ion transitions occur within an inner orbital. Because the electrons are shielded from external perturbations by the outer orbital, the optical transitions are mainly host independent. The host does affect the fine structure of the absorption and emission spectra, the non-radiative decay rates, and the relative strengths of radiative and non-radiative transitions. Two important host properties are the surrounding field it imposes on the rare-earth ion and its phonon energy, which affects the non-radiative decay rates. The detailed energy level diagram for erbium in silica is shown in Fig. 2.1. When the ions are placed in a crystalline host, the electric field of the crystalline atoms destroys the spherical symmetry thus splitting degenerated levels. This is referred to as Stark splitting. Neighboring ions experience different field distributions in the amorphous glass, which produces *inhomogeneous broadening* of the energy levels. However, *phonon coupling* causes *homogeneous broadening* that dominates at

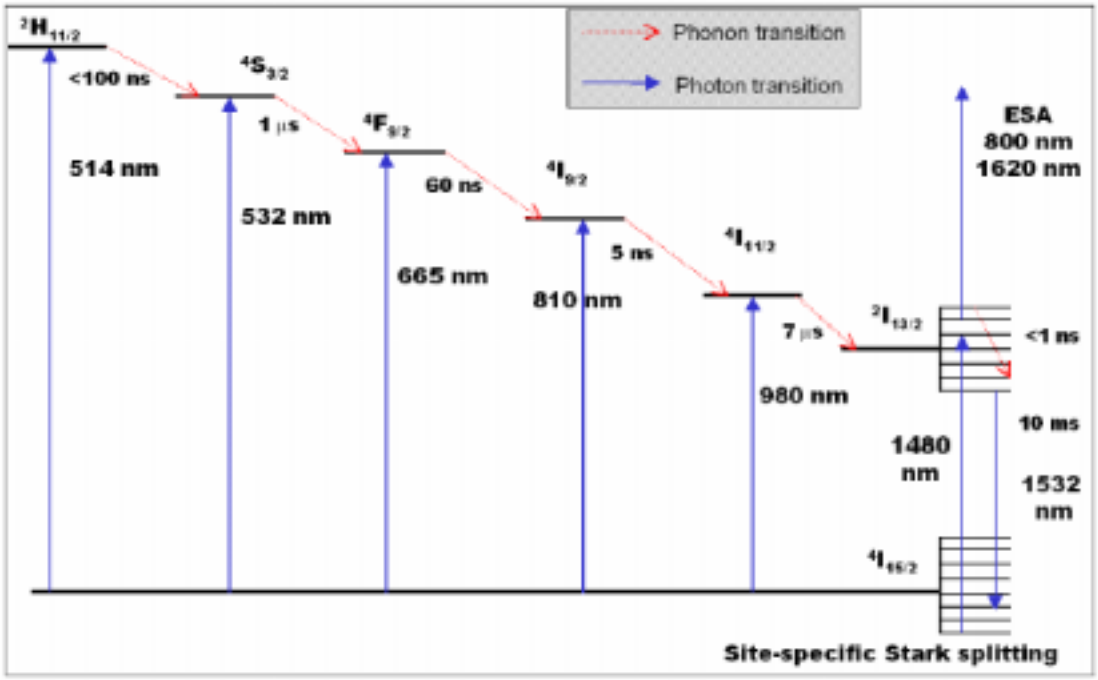

Fig. 2.1 Erbium energy levels in silica [2.3].

room temperature. Thus, the emission and absorption resonances are quite board and differ from one glass to another. Broadened energy levels are advantageous because they are insensitive to small changes in the pump and signal wavelengths. Stark splitting also allows 1480 nm pumping from the bottom of the ground level to the top of the metastable level.

EDFAs gain spectrum is mainly determined two characteristics, which are emission σ_{21} and absorption σ_{12} cross sections defined as:

$$P_{abs} = \sigma_{12} I$$

$$P_{em} = \sigma_{21} I$$

where P_{abs} and P_{em} are the amounts of light power absorbed and emitted respectively, I is the intensity of incident light. Indices 1 and 2 correspond to the energy levels E_1 and E_2 between which the transition occurs ($E_2 > E_1$). The total power change can be written as

$$\Delta P = P_{em} - P_{abs} = (N_2 \sigma_{21} - N_1 \sigma_{12}) I$$

where N_1 and N_2 are populations of the respective energy levels. The link between the emission and absorption cross section is given by McCumber relationship:

$$\sigma_{21}(\nu) = \sigma_{12}(\nu) \exp[(\varepsilon - h\nu)/kT]$$

where ε is the mean transition energy between the two manifolds involved in the transition [2.4]. An additional relationship is provided by the McCumber analysis, linking radiative lifetime and the emission cross section:

$$\frac{1}{\tau_{21}} = \frac{8\pi n^2}{c^2} \int \nu^2 \sigma_{21}(\nu) d\nu$$

where n is refractive index. The emission cross section is determined after the absorption cross sections and τ_{21} lifetime have been measured. This treatment has excellent agreement with experiment.

2.1.2 Lifetimes

The lifetime of a level is inversely proportional to the probability per unit time of the exit of an ion from that excited level. The lifetime for a given rare earth level usually follows two main decay paths, *radiative* and *nonradiative*:

$$\frac{1}{\tau} = \frac{1}{\tau_r} + \frac{1}{\tau_{nr}}$$

The radiative lifetime arises from the fluorescence from the excited level to all the levels below it. Since the radiative transitions are forbidden to first order, radiative lifetimes tends to be long, on the order of microseconds to milliseconds. In the nonradiative process, the deactivation process from the excited rare earth level is accompanied by the emission of one or several phonons (i.e., elementary vibrations of the host). The higher the number of phonons needed to bridge the energy gap, the less likely the probability of the transition. The nonradiative transition probability drops exponentially with the number of phonons required to bridge the energy gap to the next lowest level. In most cases, a lower nonradiative transition rate is desired. Typical lifetime for $^4I_{13/2}$ in erbium ranges from 7 to 14 ms depending on the host glass. The long lifetime permits the population inversion between $^4I_{13/2}$ and $^4I_{15/2}$ levels with a weak pump source.

2.1.3 Linewidths and broadening

The line width of a transition contains contributions from various effects. For a transition between two given eigenstates of a rare earth ion, the linewidth, or breath, of a transition, contains both a homogenous and inhomogeneous contribution. The *homogeneous broadening* arises from the lifetime and dephasing time of the state and depends on the both *radative* and *nonradiative* processes [2.5]. The faster the lifetime or dephasing time, the broader the state. The *inhomogeneous broadening* is a measure of the various different sites in which an ensemble of ions can be situated. With variations in the local environment of an ion, there will be shifts in the energy levels of the ion and the fluorescence or absorption observed from this collection of ions will be smeared by the inhomogeneous broadening. An inhomogeneous line is thus a superposition of a set of homogeneous lines. Such homogeneous and inhomogeneous lineshapes are depicted in Fig. 2.2.

In the presence of a strong signal that saturates the transition, the absorption or emission lineshape will be affected in a different way, depending on whether the line is homogeneously or inhomogeneously broadened. In short, one can say that in the case of homogeneous broadening, the line will saturate uniformly as the population inversion is reduced (for example, under the effect of a strong signal). On the other hand, in the case of inhomogeneous broadening, the population inversion can be “locally” affected in a subset of the entire energy space of the considered transition.

The gain spectrum then changes non-uniformly across the transition, with a “hole” in the vicinity of the energy level where the population inversion was depleted. These two different fashions of gain saturation are depicted in Fig. 2.3.

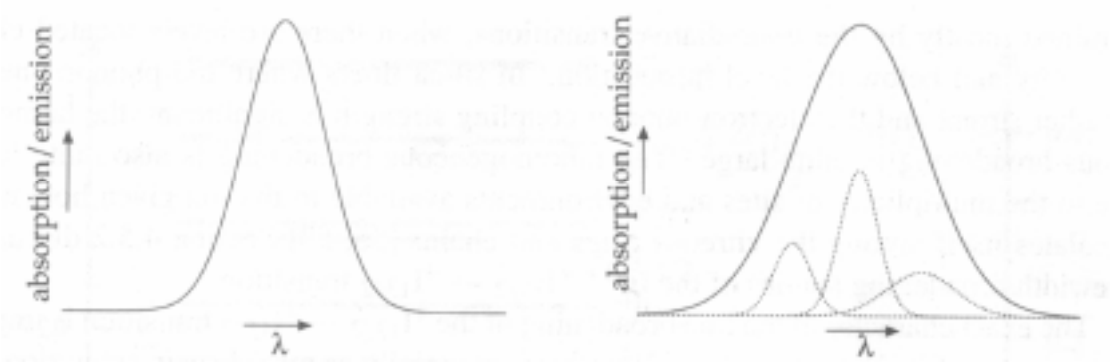

Fig. 2.2 Left: a homogeneously broadened line for a collection of ions with identical transition frequencies and lifetime. Right: inhomogeneously broadened line made up a collection of homogeneously broadened lines with different center frequencies and linewidths.

Fig. 2.3 Gain saturation for a broadened line (solid line: unsaturated gain; dotted line: saturated gain in the presence of a strong signal). Left: gain saturation for a homogeneously broadened line. Right: gain saturation for an inhomogeneously broadened line (the spectral position of the narrow band strong signal is indicated by the arrow).

In general, the larger the number of Stark components, the broader will be the total splitting of the manifold and the larger the breadth of the transition between the

manifolds. If the population redistribution between the Stark levels is fast enough (i.e., faster than the level lifetime scale over which the light signal of interest is interacting with the ion), then the entire transition will take on a homogeneously broadened character. That is, the saturation of a transition between Stark levels saturates the transitions between the other Stark levels of the multiplets.

The homogeneous broadening of a given level is determined mostly by the nonradiative transitions, when there are levels located close in energy and below the level. In silica fibers where the phonon energy is rather strong and the electron-phonon coupling strength is significant, the homogeneous broadening is quite larger. In the presence of homogeneous broadening, a strong enough signal can extract all the energy stored in the amplifier, while for an inhomogeneously broadened amplifier only the energy stored in the subset of ions interacting with the incident radiation can be extracted. Thus, homogeneously broadened amplifiers are more efficient in providing energy to a signal than inhomogeneously broadened amplifiers. On the other hand, a homogeneously broadened amplifier used in a WDM system is very susceptible to adding and dropping of wavelength channels, or their power, in that this will affect the gain and energy extraction of other channels.

2.1.4 Spectral hole burning [2.6]

A localized signal power-dependent spectral gain depression is referred to as spectral hole burning (SHB) [2.7]. SHB occurs in EDFAs when a strong signal reduces the average ion population contributing to gain at a particular wavelength in excess of the global reduction.

SHB is relatively small in EDFAs since these amplifiers are predominantly homogeneously broadened. A homogeneously broadened amplifier has the property that an input signal at any wavelength in the amplification band can equally access the total energy stored within the amplifier. Homogeneous broadening in EDFAs is caused by the rapid transport of energy across the different Stark-broadened lines within a specific manifold [2.8]. This tends to reduce the extent of the SHB. The presence of phonons (heat exchange) is responsible for the EDFA homogeneous broadening.

Research has shown that at room temperature, SHB is relatively small for EDFAs with a dependency of ~0.3 dB per dB increase in gain compression [2.9]. The effect of

SHB tends to be more significant in the 1530 nm wavelength region than 1550 nm region.

2.1.5 Pump sources and configurations

Erbium-doped fiber amplifiers are traditionally pumped with either 980 nm or 1480 nm laser diodes, which correspond to exciting $^4I_{11/2}$ and $^4I_{13/2}$ levels respectively. The first case can be described by a three-level laser model whereas the second case is a quasi-three-level system. In the last case, there are two levels in the light generation process, however each of them is a collection of Stark sublevels. Thus the pump light excites the ions from the lower sublevels of $^4I_{15/2}$ to the upper sublevels of $^4I_{13/2}$, while the radiation is emitted when the ion relaxes from lower sublevels of $^4I_{13/2}$ to the higher sublevels of $^4I_{15/2}$. The radiation wavelength is then longer than pump wavelength. The transitions between sublevels within each level are nonradiative. The 980 nm pump source allows to decrease the noise figure because the decay out of $^4I_{11/2}$ is very slow to effectively populate the upper state of the amplifying transition. Hence, the improvement of the noise figure is achieved at the expense of gain efficiency [2.10].

Three different pump configurations are possible for a length of erbium-doped fiber: copropagating pump and signal, counterpropagating pump and signal, and bidirectional pump. The principal difference between these configurations is in the ASE pattern and inversion profile. For a small signal gain, co- and counter-propagating schemes yield the same gain since pump patterns are the mirror images of each other and the average population inversion is the same. However, ASE power levels and spectra do differ at the output. When the signal power is increased, so that it can affect seriously the inversion, pump direction becomes important for signal gain. In general, the most advantageous situation is when the signal is strong where the inversion is high so that the signal, not the ASE, will deplete the gain. If we contrast co- and counter-propagating schemes in the aspect of noise figure for moderate and small signals, copropagating pump results in lower noise figure. There are two reasons for this behavior. First, forward ASE is smaller in copropagating schemes. Second, when signals enter the amplifier with counterpropagating pump, the inversion at the beginning is low so that signal may even experience some loss, which

contributes to the SNR degradation. Still, bidirectional pump gives better gain and noise performance.

Typically, two types of pump sources are used in modern EDFAs: 980 nm and 1480 nm laser diodes. The choice of 1480 nm yields a better power conversion efficiency, given a larger number of photons available at 1480 nm for a specific power, compared to 980 nm light. However, the noise figure is smaller with 980 nm pump since it can offer higher inversion population. The multistage amplifiers have been used in practice to achieve the high power conversion efficiency and low noise figure. It is often advantageous to pump the first stage with 980 nm light and the second stage with 1480 nm light. The 980 nm pumping has the benefit of low noise figure at the input portion, while 1480 nm pumping offers much higher optical conversion efficiency for the power portion. The most simple of the two-stage amplifiers contain two sections of erbium-doped fiber, separated by an isolator or a filter. The isolator eliminates the backward traveling ASE from the second portion that would otherwise deplete inversion in the first section. The first stage needs to be well-inverted so that a moderate amount of gain is obtained with minimum noise figure. The second stage acts as a power amplifier.

2.1.6 Principle of long-wavelength band (L-band) EDFA [2.11]

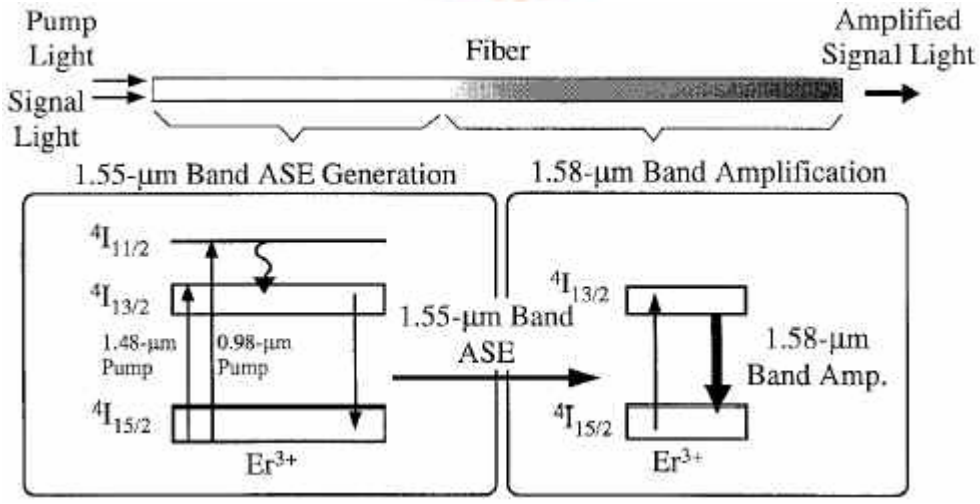

Fig. 2.4 Schematic diagram of 1.58-μm band amplification.

Fig. 2.4 shows a schematic diagram of 1.58-μm band amplification. 1.55-μm band amplified spontaneous emission (ASE) is generated by 0.98-μm or 1.48-μm band pump light at the input portion of the fiber. The ASE is absorbed at the output portion, so 1.58-μm band amplification is realized. A long Er^{3+}-doped fiber is needed because the gain coefficient in the 1.58-μm band is smaller than that in the 1.55-μm band.

2.2 Gain and noise figure measurement [2.12],[2.13]

2.2.1 Gain and noise figure

The gain of an amplifier is expressed as the ratio between the input signal level and the output signal level, typically expressed in dB.

$$Gain(dB) = 10 \times \log_{10}\left(\frac{P_{signal-out}}{P_{signal-in}}\right) \tag{2-1}$$

The degradation of the signal-to-noise ratio (SNR) after passage through an optical amplifier is quantified in terms of the noise factor, *F*, defined as

$$F = \frac{SNR_{in}}{SNR_{out}} \tag{2-2}$$

The input SNR is defined to be that from a shot-noise-limited source. The shot-noise-limited input reference is critical to the definition. If an optical source with a large amount of intensity noise were used to measure the noise figure of an amplifier, the amplified source noise would dominate over the amplifiers own noise contribution and lead to an erroneous noise figure of 0 dB, in other words, no observed SNR degradation caused by the amplifier.

A commonly used definition of noise factor is the signal-spontaneous beat noise density depending on the product of the ASE density in the same polarization state as the signal and the amplified optical signal. Therefore, the noise factor is the sum of the signal-spontaneous beat noise and shot noise.

$$F = F_{sig-sp} + F_{shot} = \frac{2\rho_{ASE}}{Ghv} + \frac{1}{G} \tag{2-3}$$

$$\rho_{ASE} = n_{sp}(G-1)hv$$

$$n_{sp} = \frac{N_2}{N_2 - \frac{\sigma_a(\lambda)}{\sigma_e(\lambda)}N_1} \quad ; n_{sp} \text{ is inversion factor}$$

where the ASE spectral density ρ_{ASE} and the gain G can be measured using the time domain extinction technique. Here, The noise figure (NF) is the noise factor expressed in decibel units:

$$NF = 10 \times \log_{10}(F) \tag{2-4}$$

2.2.2 Time Domain Extinction Technique

In this dissertation, we use the time domain extinction technique to measure the gains and noise figures. This method takes advantage of the slow gain dynamics of the EDFA to reduce the effect of source spontaneous emission (SSE) on the noise figure measurement [2.13]-[2.16]. When the EDFA is driven into saturation, the gain and the amplified spontaneous emission (ASE) depend on the average incident signal intensity. When the signal is pulsed-off, the EDFA gain recovers to a new steady state level. The recovery time is slow enough (microsecond time-scales) such that the ASE from the amplifier may be measured before it changes appreciably. Since the signal and SSE are no longer present, the measured ASE corresponds to the actual ASE generated by the optical amplifier. The signal is then pulsed back on and the process repeats.

A measurement setup for this technique is shown in Fig. 2.5. When the input switch is closed as shown in Fig. 2.5(a), the amplifier is illuminated by signal and noise. In Fig. 2.5(b), the input switch is opened extinguishing the signal and output switch closes. This enables the optical spectrum analyzer (OSA) to sample the ASE produced by the amplifier. When the gating rate is slow compared to the gain recovery time of the amplifier, the response is as shown in Fig. 2.6(a). Energy storage in the amplifier causes a signal transient as the signal is gated into the amplifier operating in the small signal regime [2.13],[2.17]. The flat portion of the waveform following the transient is the steady state condition. If the ASE is measured soon after the signal is gated off, it will be the same ASE generated in the presence of signals. When the gating rate is faster than the gain recovery time of the amplifier, the response is as shown in Fig. 2.6(b). In this case the effective input power that determines the amplifier saturation state is the time average of the gated signal. The ASE waveform is triangular with an offset during the signal-on interval due to additive effect of the SSE. If the ASE is sampled halfway through the positive going slope as shown, the ASE will correspond to the ASE generated by the amplifier in the presence of the average signal power. The error due to gain recovery varies linearly with pump power [2.13]. For EDFAs,

pulse repetition rates of 25 kHz or more are typically used.

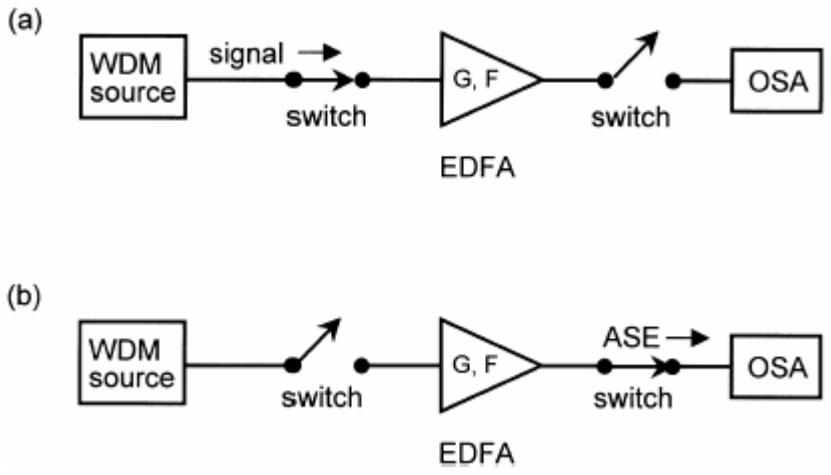

Fig. 2.5 Time-domain extinction method for amplifier ASE measurement. (a) Signal is setting amplifier saturation state. (b) Signal disconnected, OSA measures ASE.

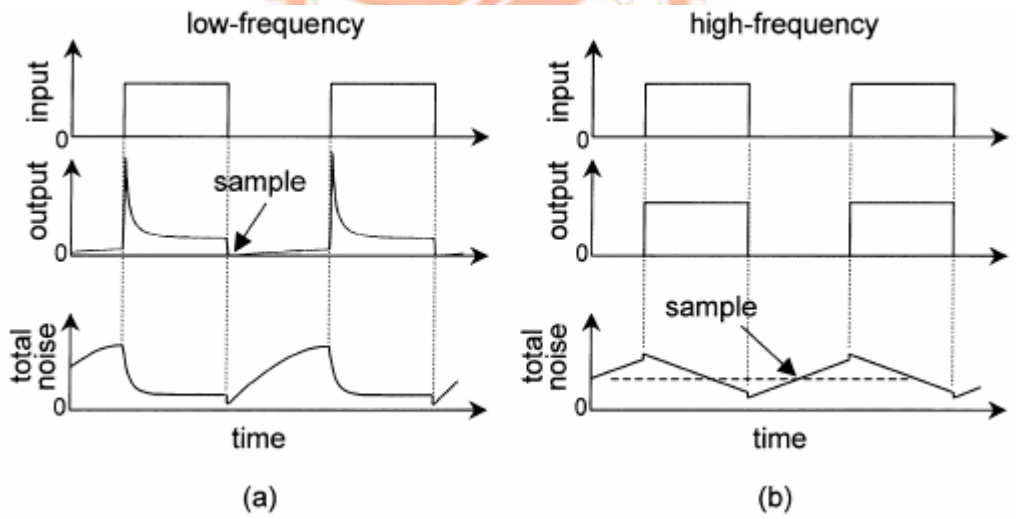

Fig. 2.6 Signal and ASE diagrams for domain extinction method for amplifier. (a) Low frequency regime. (b) High frequency regime.

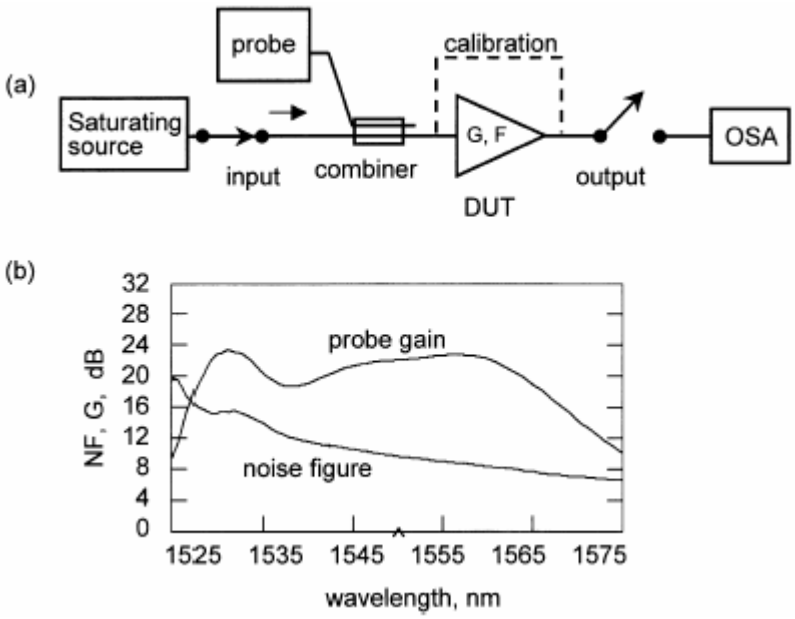

Fig. 2.7 (a) Dynamic gain and noise figure measurement setup. (b) Measurement with a saturation wavelength of 1550 nm.

The extinction ratio of the switches shown in Fig. 2.5 is important. Multiple switch stages may be required to obtain complete suppression of the signal. When the depth of the extinction is not sufficient to completely reject the signal, interpolation is used to estimate the ASE at the signal wavelength.

With the addition of a small signal probe, a swept-wavelength characterization of the EDFA gain spectrum can be performed [2.13],[2.18]. This permits gain tilt characterization for DWDM applications by measuring the variation in gain between the test laser wavelengths. Fig. 2.7 shows a typical measurement of gain and noise figure using this technique. In Fig. 2.7(a), the pulsed edge-emitting LED (EELED) probe provides a broadband stimulus from a wavelength of 1525 to 1575 nm. Three measurements are performed during the time interval when the saturating source is gated off:

1. Calibration: small-signal probe power versus wavelength with EDFA bypassed: $P_{cal}(\lambda)$
2. Small-signal probe power and ASE power versus wavelength with EDFA inserted: $P_1(\lambda)$
3. ASE power versus wavelength with EDFA inserted (probe not sampled): $P_2(\lambda)$

The amplifier gain is calculated using:

$$G(\lambda) = \frac{P_1(\lambda) - P_2(\lambda)}{P_{cal}(\lambda)}$$

Fig. 2.7(b) shows a measured noise figure using this technique. The noise factor was calculated using Eq. (2-3) with $\rho_{ASE}(\lambda) = P_2(\lambda)/2B_0$, where B_0 is the effective noise bandwidth of the OSA.

2.2.3 Noise factor of cascaded components

In this section, we consider the noise factor of a cascade of optical components. The main objective of this section is to develop an expression for the total noise figure of a cascade of noisy components. Each stage of amplification adds additional noise to the signal as well as amplifying the noise generated from previous stages. This process is illustrated in Fig. 2.8, which shows a cascade of *N* amplifiers in which the *i*th stage has gain G_i and ASE spectral density ρ_{ASEi}. The ASE from the first amplifier is multiplied by the gain of the second stage that in turn adds additional ASE. This process continues to the *N*th amplifier stage. The ASE density ρ_{ASE}^{c} at the output of the cascade is

$$\rho_{ASE}^{c} = \rho_{ASE1}(G_2 G_3 \cdots G_N) + \rho_{ASE2}(G_3 G_4 \cdots G_N) + \cdots\cdots + \rho_{ASEN-1} G_N + \rho_{ASEN} \qquad (2\text{-}5)$$

Given the gain, *G*, of each amplifier stage and the ASE contribution at each stage, the total ASE can be calculated. The signal-spontaneous noise factor $F_{\text{sig-sp}}$ for the amplifier is often used as a figure of merit indicating the amount of ASE generated by the amplifier per unit gain. With knowledge of the gain, *G*, and noise factor $F_{\text{sig-sp}}$, the total ASE density, ρ_{ASE} can be calculated. The noise figure of a cascade of amplifiers can then be determined in a straightforward manner as follows.

Dividing Eq. (2-5) by the total gain of the cascade, $G_{Total} = G_1 G_2 \cdots G_N$, and multiplying by the quantity $(2/h\nu)$ gives the effective signal-spontaneous noise factor of the cascade:

$$\frac{2\rho_{ASE}^{c}}{h\nu G_{Total}} = \frac{2\rho_{ASE1}}{h\nu G_1} + \frac{2\rho_{ASE2}}{h\nu G_1 G_2} + \cdots\cdots + \frac{2\rho_{ASEN-1}}{h\nu G_1 G_2 \cdots G_{N-1}} + \frac{2\rho_{ASEN}}{h\nu G_{Total}} \qquad (2\text{-}6)$$

We find from Eqs. (2-3) and (2-6) that the total signal-spontaneous noise factor F_{sig-sp}^{c} for a cascade of N stages of amplification is

$$F_{sig-sp}^{c} = F_{sig-sp,1}^{c} + \frac{F_{sig-sp,2}^{c}}{G_1} + \frac{F_{sig-sp,3}^{c}}{G_1 G_2} + \cdots\cdots + \frac{F_{sig-sp,N}^{c}}{G_1 G_2 \cdots\cdots G_{N-1}}$$

where $F_{sig-sp,N}$ is the noise factor of the *N*th stage. Consequently, the noise factor of a multi-stage amplifier is dominated by the noise factor of the first stage.

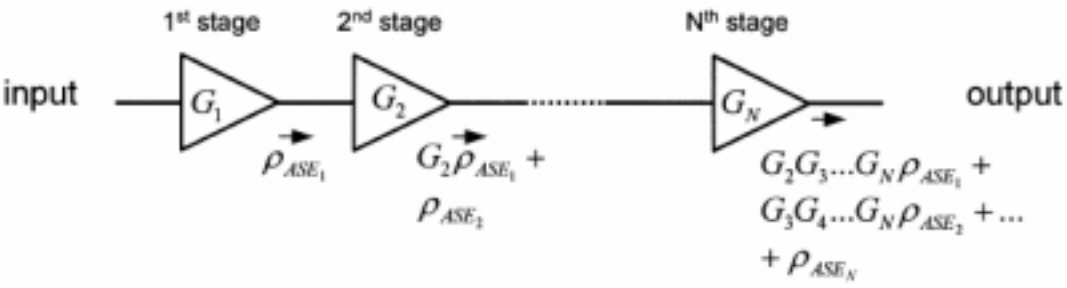

Fig. 2.8 Cascade of optical amplifiers leading to an accumulation of ASE.

2.3 Characteristics of all-optical gain-clamped EDFA

2.3.1 Gain transient [2.19]

The time dynamics of the gain process in an erbium-doped fiber amplifier give rise to transient effects. These effects can manifest themselves when a non-steady-state signal is amplified. The classic examples of such a situation are

- a single-channel signal is modulated in time.
- one or more channels are added to a collection of WDM channels.
- one or more channels are removed from a collection of WDM channels.

In digital signal transmission with intensity modulation, the signal is modulated at the bit rate. In most cases, the bit rate is much higher than the frequency with which the erbium ion gain dynamics can respond, so that the signal appears to be essentially steady state. The slow gain dynamics arise from the long upper-state lifetime of the erbium ion as well as from the rather long stimulated lifetimes. This latter lifetime is long for the typical power levels of the pump and signal in the erbium-doped fiber. When the modulation frequency is low enough on the order of the characteristic

response time of the erbium gain dynamics, transient effects begin to appear [2.20]. Fig. 2.9 shows an example in which the amplifier gain at λ_{probe} was compressed by 5 dB [2-21]. At the leading edge of the strong signal, there is a gain overshoot as the inversion drops down to a steady-state value, corresponding to a balance between the signal stimulated emission rate and the pumping rate. The front of the pulse initially has more gain as it sees a higher inversion. Reduction of the population inversion caused by the modulated laser appears as an exponential decrease of the probe signal output to a lower steady-state value. In this case, the time constant is 110 μs and the gain-recovery time constant corresponding to the dropping of the strong signal is 300 μs.

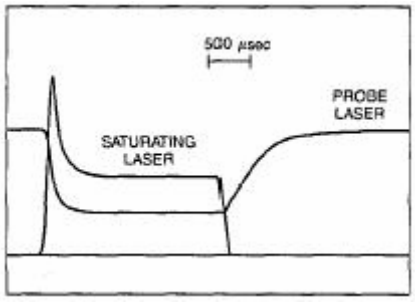

Fig. 2.9 Amplified signals showing the gain saturation and recovery during pulse amplifications. The pump power is 210 mW, the saturating pulse power is 34.4 μW at 1531 nm, and the cw pulse signal signal 3.48 μW at 1537.5 nm.

2.3.2 Choice of feedback lasing wavelength [2.22]

The common goal of the gain clamping by an all-optical feedback loop is that the maximum value of the power excursions of the surviving channel should be less than a fraction of a dB for any possible change in channel loading. These power excursions have two contributions: a static contribution owing to the spectral hole burning (SHB), and a dynamic contribution owing to the relaxation oscillations in laser. Fig. 2.10 shows transient response of the surviving signal output power, for three different lasing wavelengths, when the 1557.8 nm signal is modulated on and off, corresponding to the worst case scenario: addition and loss of seven of eight WDM channels. For a given lasing wavelength (λ_l), the attenuator loss in the feedback loop is adjusted to maintain the same output power for the surviving channel.

At λ_l = 1532 nm, Fig. 2.10(a), the laser AGC suppresses transients in the surviving

channel, but not completely. This failure of the laser AGC arises from spectral hole burning, i.e., inhomogeneity of the erbium gain medium. The transition between these two gain levels requires on the order from 100 μs to 200 μs, reflecting the slow gain dynamics of the erbium gain medium. Note that the spikes arising due to relaxation oscillation in the laser do not undershoot and/or overshoot the steady-state values for lasing wavelengths near 1530 nm. This indicates that when the lasing wavelength, for the set of wavelengths considered here, is not close to the spectral band occupied by signal wavelengths, the steady-state power excursions arising from spectral hole burning are dominant.

At λ_l = 1540 nm, as can be seen from Fig. 2.10(b), relaxation oscillations in the laser gives rise to fast oscillations in the surviving signal power resulting in transients which undershoot the lower gain level and overshoot the higher gain level. On the other hand, residual power excursions from SHB become smaller, as λ_l approaches the signal wavelength. The residual power excursions resulting from the static component due to the spectral hole burning, and the dynamic component due to the relaxation oscillations in laser are both present.

At λ_l = 1555 nm, as can be seen from Fig. 2.10(c), relaxation oscillations in laser give rise to the dominant residual power excursions in the surviving signal. As expected, residual power excursions from SHB are completely absent as the lasing wavelength closely approaches the spectral band occupied by signal wavelengths. Note that both the frequency and amplitude of the relaxation oscillations are different when channels are added or lost. Both the frequency and amplitude of the transient power excursions of the surviving channel are lower in the case of adding channels versus that of losing channels. Dropping of channels results in much more severe effects on the surviving channels.

The above discussions indicate that there is a tradeoff in selecting the lasing control wavelength to minimize impairments from SHB and relaxation oscillations; a lasing wavelength cannot be chosen, which avoids both impairments. Note, however, that the main reason for system impairments stems from spikes arising due to relaxation oscillation in the laser and the associated strong undershoot and/or overshoot from the steady-state values. Therefore, system impairments arising from static power excursions are less significant than those arising from dynamic power excursions.

This means that the effects of the inhomogeneity of the erbium gain spectrum on the transient response may be negligible for a single amplifier but will compound in large networks of concatenated EDFAs.

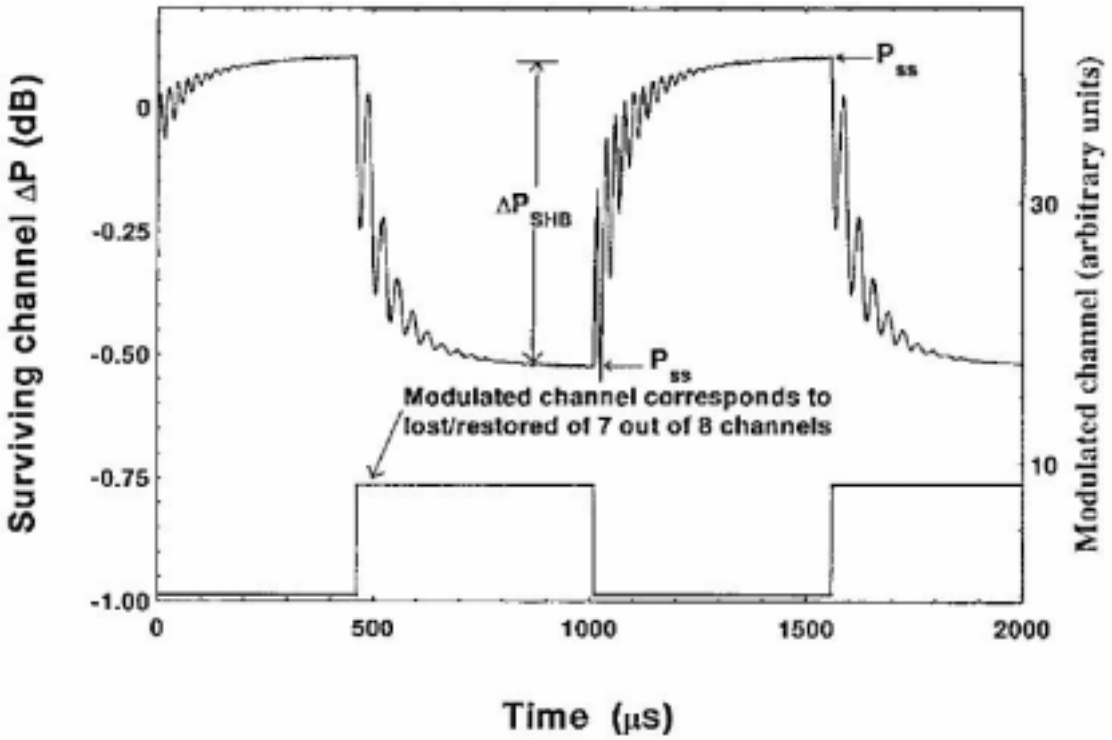

(a)

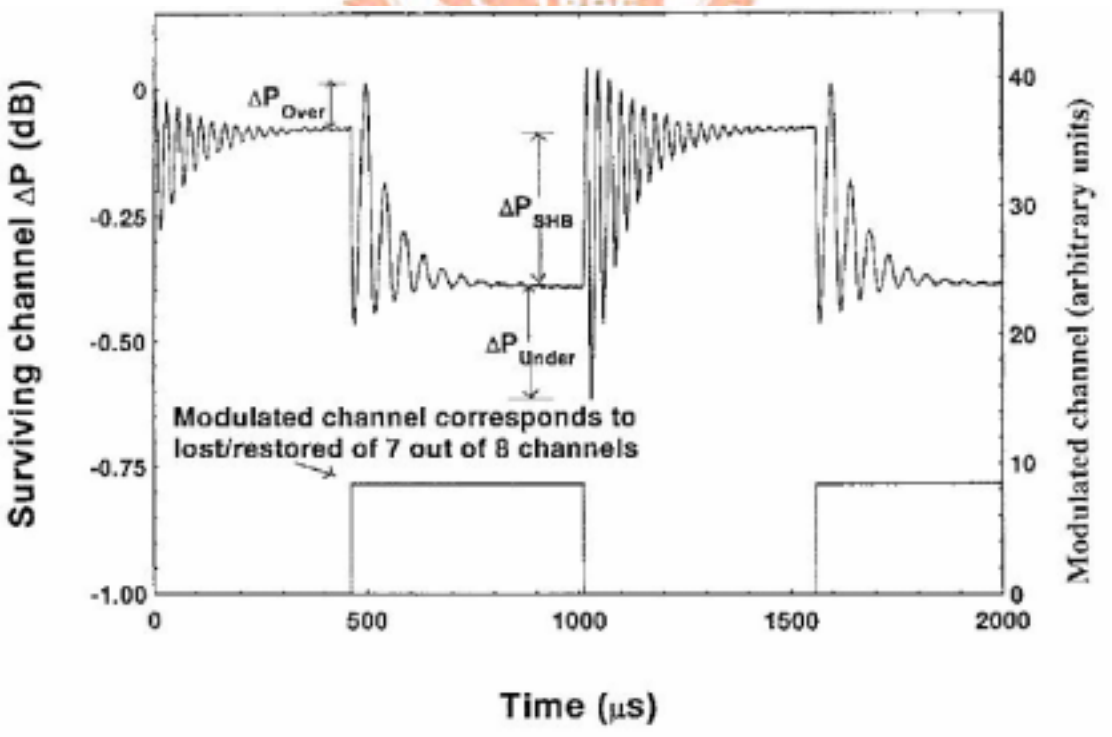

(b)

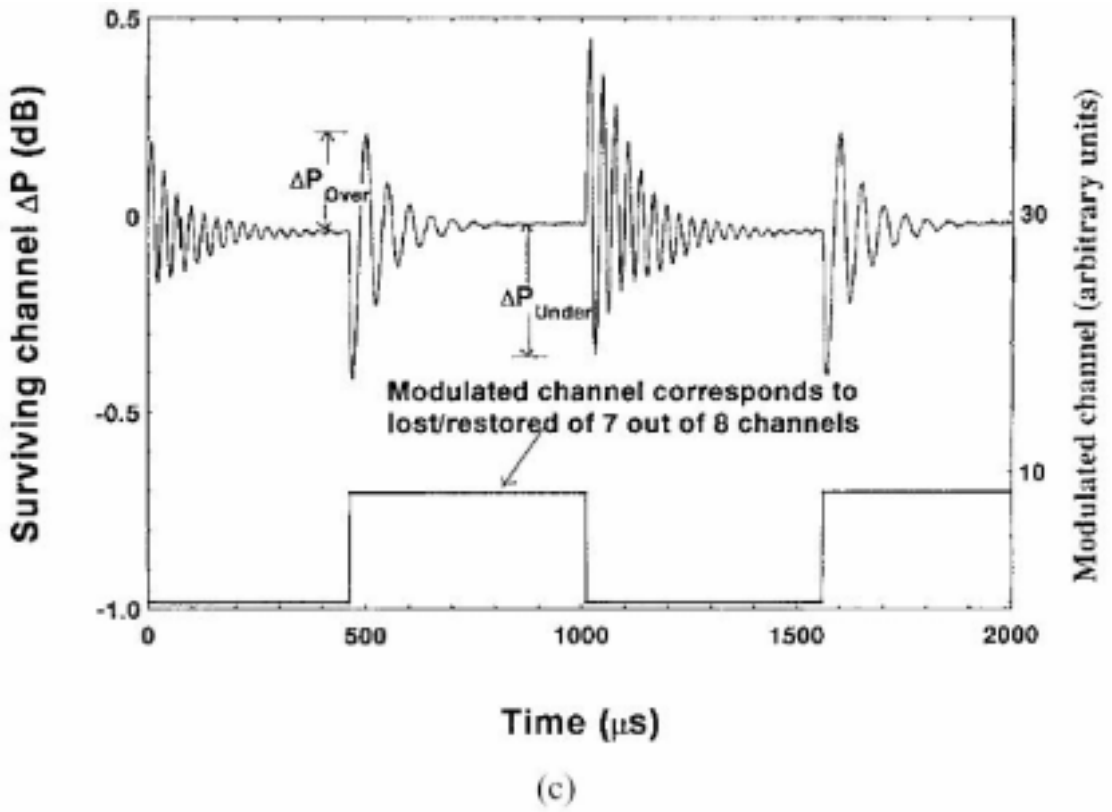

Fig. 2.10 Transient response of surviving channel output power to dropping/adding seven of eight channels. (a) The amplifier operated at 15 dB gain compression, the lasing wavelength is 1532 nm, (b) the same as (a) except that the lasing wavelength is 1540 nm, and (c) the same as (a) except that the lasing wavelength is 1555 nm.

2.3.3 Number of channels dropped/added [2.22]

For a given attenuator loss, both the frequency and amplitude of the power excursions experienced by the surviving channels are a function of the number of channels in the system. Fig. 2.11 shows the dynamics of the surviving channel when four and seven channels are switched, respectively. It can be seen that as the number of switched channels increase, both the frequency and amplitude of the power excursions experienced by the surviving channels increase. Furthermore, the power in the remaining channel increases when four channels are dropped, but decreases when seven channels are dropped. This is due to the fact that the attenuator loss was adjusted to a slightly lower value in the case of dropping seven channels. Fig. 2.12 shows the simulation results corresponding to the experimental results shown in Fig.

2.11. The simulation results have good qualitative agreement with the experiments and confirm the fact that as the number of switched channels increase, both the frequency and amplitude of the power excursions experienced by the surviving channels increase.

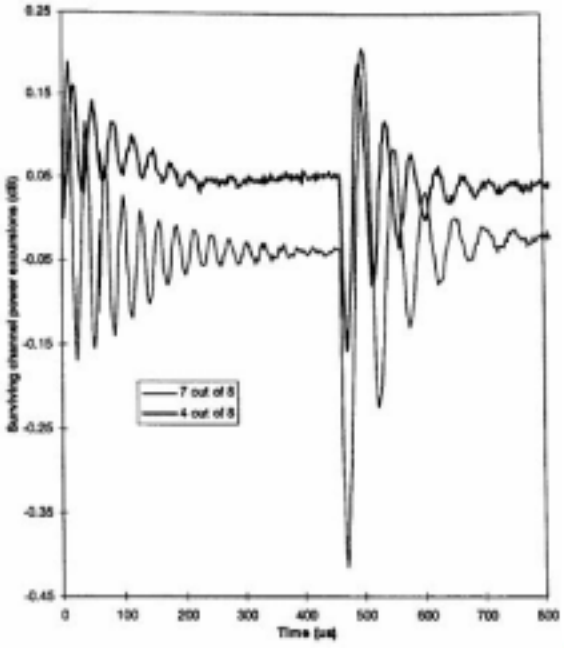

Fig. 2.11 Transient response of surviving channel output power when 4 and 7 channels are switched, respectively.

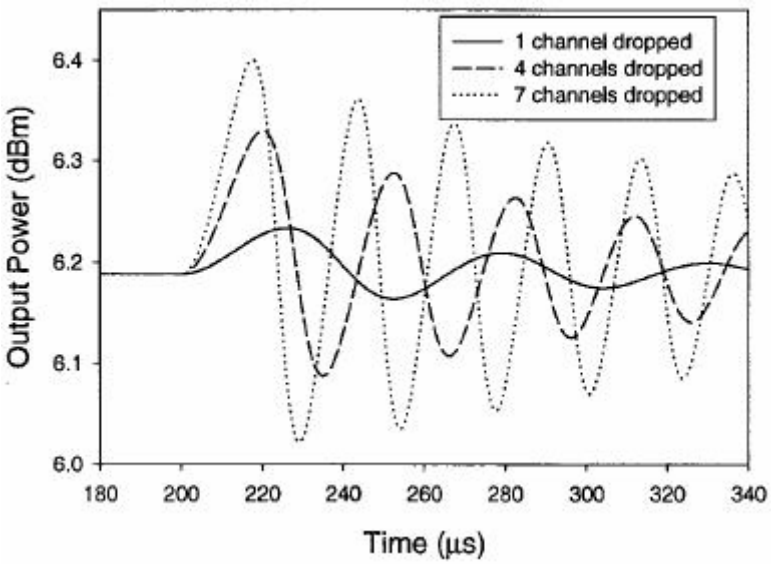

Fig. 2.12 Simulation results corresponding to the experimental results shown in Fig. 2.11.

References

[2.1] P. C. Becker, N. A. Olsson, and J. R. Simpson, *Erbium-Doped Fiber Amplifiers. Fundamentals and Technology*. Academic press, pp. 99-110, 1999.

[2.2] O. V. Sinkin, "Erbium-doped fiber amplifier technology in optical fiber communications systems," *ENEE 785 class report*, 2001.

[2.3] Introduction, Technical Background and Tutorial of OptiAmplifier (version 3.0), pp.23, 2001.

[2.4] D. E. McCumber, "Theory of phonon-terminated optical masers," *Phys Rev.* 134, pp. A299-A306, 1964.

[2.5] P. W. Milonni, and J. H. Eberly, *Lasers*, Wiley, New York, 1988.

[2.6] D. Derrickson, "Characterization of erbium-doped fiber amplifier," in *Fiber Optic Test and Measurement*, pp. 531, Prentice-Hall, Eaglewood Cliffs, NJ, 1998.

[2.7] E. Desurvire, J. L. Zyskind, and J. R. Simpson, "Spectral gain hole-burning at 1.53 μm in erbium-doped fiber amplifiers," *IEEE Photon. Technol. Lett.*, vol.2, pp. 52-54, 1990.

[2.8] G. R. Walker, "Gain and noise characterization of erbium-doped fiber amplifiers," *Electron. Lett.*, vol.27, pp. 744-745, 1991.

[2.9] A. K. Srivastava, J. L. Zyskind, J. W. Sulhoff, J. D. Evankow, and M. A. Mills, "Room temperature spectral hole-burning in erbium-doped fiber amplifiers," *in OFC'96 Technical Digest, Optical Fiber Communication Conference, Technical Figest Series* vol.2, pp. 33-34, 1996.

[2.10] M. Yamada, Y. Ohishi, T. Kanamori, H. Ono, S. Sudo, and M. Shimizu, "Low-noise and gain-flattened fluoride-based Er3+-doped fibre amplifier pumped by 0.97 μm laser diode," *Elect. Lett.*, vol.33, pp. 809-810, 1997.

[2.11] H. Ono, M. Yamada, T. Kanamori, S. Sudo, and Y. Ohishi, "1.58- μ m band gain-flattened erbium-doped fiber amplifiers for WDM transmission systems," *J. Lightwave. Technol.*, vol.17, pp. 490-496, 1999.

[2.12] D. M. Baney, P. Gallion, and R. S. Tucker, "Theory and measurement techniques for the noise figure of optical amplifiers," *Optical Fiber Technology*, vol.6, pp. 122-154, 2000.

[2.13] D. Derrickson, "Characterization of erbium-doped fiber amplifier," in *Fiber Optic Test and Measurement*, chapter 13, Prentice-Hall, Eaglewood Cliffs, NJ,

1998.

[2.14] S. Poole, “Noise figure measurement in optical fibre amplifiers,” in *Symposium on optical fiber measurements*, NIST Technical Digest, pp. 1-6, 1994

[2.15] K. Bertilsson, P. A. Andrekson, and B. E. Olsson, “Noise figure of erbium doped fiber amplifiers in the saturated regime,” *IEEE Photon. Technol. Lett.*, vol.6, pp. 199-201, 1994.

[2.16] D. M. Baney, and J. Dupre, “Pulsed- source technique for optical amplifier noise figure measurement,” *European Conference on Communications, ECOC’92*, paper WeP2.11, Berlin, 1992.

[2.17] H. Desurvire, *Erbium Doped Fiber Amplifiers, Principles and Application*, Wiley, New York, 1994.

[2.18] H. Cjou, and J. Stimple, “Inhomogeneous gain saturation of erbium-doped fiber amplifiers,” in *Optical Amplifiers and Their Applications, OAA’95*, paper ThE1-1, Optical Society of America, Washington, DC, 1995.

[2.19] P. C. Becker, N. A. Olsson, and J. R. Simpson, *Erbium-Doped Fiber Amplifiers. Fundamentals and Technology*. Academic press, pp. 363-366, 1999.

[2.20] E. Desurvire, “Analysis of transient gain saturation and recovery in erbium-doped fiber amplifiers,” *IEEE Photon. Technol. Lett.*, vol.1, pp. 196-199, 1989.

[2.21] C. R. Giles, E. Desurvire, and J. R. Simpson, “Transient gain and cross talk in erbium-doped fiber amplifiers,” *Opt. Lett.*, vol.14, pp. 880-882, 1989.

[2.22] G. Luo, J. L. Zyskind, J. A. Nagel, and Mohamed A. Ali, “Experimental and theoretical analysis of relaxation-oscillations and spectral hole burning effects in all-optical gain-clamped EDFA’s for WDM networks,” *J. Lightwave. Technol.*, vol.16, pp. 527-533, 1998.